AGU PUBLICATIONS

JGR

Journal of Geophysical Research: Atmospheres

RESEARCH ARTICLE
10.1002/2016JD025273

Special Section:
The Arctic: An AGU Joint Special Collection

Multiyear study of the dependence of sea salt aerosol on wind speed and sea ice conditions in the coastal Arctic

N. W. May[1], P. K. Quinn[2], S. M. McNamara[1], and K. A. Pratt[1,3]

[1]Department of Chemistry, University of Michigan, Ann Arbor, Michigan, USA, [2]Pacific Marine Environmental Laboratory, National Oceanic and Atmospheric Administration, Seattle, Washington, USA, [3]Department of Earth and Environmental Sciences, University of Michigan, Ann Arbor, Michigan, USA

Key Points:
- Local sea ice coverage and wind speed are controlling factors for Arctic sea salt concentrations
- Sea salt aerosol is produced from sea ice leads at wind speeds > 4 m/s
- The influence of long-range transported sea salt aerosol was greatest during periods of lower winds and increased sea ice coverage

Supporting Information:
- Supporting Information S1

Correspondence to:
K. A. Pratt,
prattka@umich.edu

Citation:
May, N. W., P. K. Quinn, S. M. McNamara, and K. A. Pratt (2016), Multiyear study of the dependence of sea salt aerosol on wind speed and sea ice conditions in the coastal Arctic, *J. Geophys. Res. Atmos.*, *121*, 9208–9219, doi:10.1002/2016JD025273.

Received 25 APR 2016
Accepted 25 JUL 2016
Accepted article online 29 JUL 2016
Published online 13 AUG 2016

Abstract Thinning of Arctic sea ice gives rise to ice fracturing and leads (areas of open water surrounded by sea ice) that are a potential source of sea salt aerosol. Atmospheric particle inorganic ion concentrations, local sea ice conditions, and meteorology at Barrow, AK, from 2006 to 2009, were combined to investigate the dependence of submicron (aerodynamic diameter $< 1\ \mu m$) and supermicron (aerodynamic diameter 1–10 μm) sea salt mass concentrations on sea ice coverage and wind speed. Consistent with a wind-dependent source, supermicron sea salt mass concentrations increased in the presence of nearby leads and wind speeds greater than $4\ m\ s^{-1}$. Increased supermicron and submicron sea salt chloride depletion was observed for periods of low winds or a lack of nearby open water, consistent with transported sea salt influence. Sea salt aerosol produced from leads has the potential to alter cloud formation, as well as the chemical composition of the Arctic atmosphere and snowpack.

1. Introduction

Rapid sea ice loss is dramatically changing the Arctic surface [*Serreze and Stroeve*, 2015]. Mean September coverage of Arctic sea ice decreased by $-13.3\%\ decade^{-1}$ for the period of 1979–2014 [*Serreze and Stroeve*, 2015], and complete summertime loss of sea ice is expected within 50 years [*Overland and Wang*, 2013]. In the winter-spring, the Arctic is becoming increasingly dominated by first-year sea ice cover [*Maslanik et al.*, 2011]. Thinner first-year sea ice is less structurally stable and more prone to fracturing, likely resulting in the formation of leads (transient areas of open water surrounded by sea ice), as well as more pancake ice [*Stroeve et al.*, 2012]. Increasing sea salt aerosol production is expected from the newly exposed ocean surface [*Browse et al.*, 2014; *Struthers et al.*, 2011]. Sea ice loss is also expected to increase the emissions of marine primary organic aerosol and dimethyl sulfide, as well as lead to changes in aerosol processing and removal in the Arctic boundary layer through changing meteorology [*Browse et al.*, 2014].

Atmospheric aerosols represent the largest source of uncertainty in global radiative forcing predictions [*Boucher et al.*, 2013]. An increase in sea salt aerosol emissions will increase Arctic aerosol optical depth, increasing the magnitude of aerosol direct radiative forcing (cooling) [*Struthers et al.*, 2011]. Sea salt aerosols can also indirectly alter radiative forcing by acting as cloud condensation nuclei (CCN) [*Wise et al.*, 2009]. Simulations by *Browse et al.* [2014] suggested that the CCN response to increased sea salt aerosol from the Arctic Ocean is weak due to efficient scavenging of particles and decreased new particle formation from a greater condensation sink. However, the predicted CCN response was spatially nonuniform, with coastal Arctic regions predicted to have a larger CCN response than the central Arctic Ocean [*Browse et al.*, 2014]. Further, deposition of sea salt aerosol to the snow surface contributes to springtime atmospheric reactive bromine chemistry and ozone depletion [*Pratt et al.*, 2013; Simpson *et al.*, 2005]. However, due to limited Arctic aerosol measurements, the contributions and radiative impacts of sea salt aerosol under changing sea ice conditions are uncertain.

Under open ocean conditions, sea salt aerosol mass concentrations typically increase with increasing wind speed [*Lewis and Schwartz*, 2004] and decreasing water temperature [*Salter et al.*, 2015]. Airborne sea salt aerosol particles are formed by two distinct processes when bubbles on the seawater surface burst [*Blanchard and Woodcock*, 1957]. The fragmentation of the top of the bubble membrane produces film drops. After the bubble membrane top bursts, droplets of water are flung upward from the bubble bottom,

producing jet drops. Particles result from film and jet drops after evaporation, with film drops mainly resulting in submicron particles and jet drops generally resulting in supermicron particles [*O'Dowd et al*., 1997]. Over the open ocean, the bubble-bursting production of sea salt aerosol is driven by wind-induced wave breaking that entrains air underneath the ocean surface. However, there is still uncertainty regarding the mechanism of aerosol production from leads. *Nilsson et al*. [2001] and *Leck et al*. [2002] measured wind-dependent number fluxes of particles, likely produced through the bubble-bursting mechanism, from open leads at a rate ~10 times less than the open ocean, which was attributed to the decreased fetch over the open leads. However, *Nilsson et al*. [2001] found that an additional particle emission mechanism was needed to explain the particle number fluxes at low wind speeds. Studies conducted under lower wind speed conditions have proposed emission mechanisms, including the transport of bubbles to the surface by increased turbulence caused by supercooling conditions [*Grammatika and Zimmerman*, 2001], gas released from melting ice [*Leck and Bigg*, 1999; *Nilsson et al*., 2001], phytoplankton respiration [*Johnson and Wangersky*, 1987], and a surface heat flux-driven mechanism [*Norris et al*., 2011].

Sea salt aerosol is a significant contributor to Arctic particle mass [*Quinn et al*., 2002]. Given the impacts of sea salt aerosol on climate and the changing sea ice surface, it is imperative to evaluate the contribution of sea salt aerosol produced from leads. Previous Arctic spring [*Radke et al*., 1976; *Scott and Levin*, 1972] and summer [*Held et al*., 2011a; *Held et al*., 2011b; *Leck and Persson*, 1996; *Leck and Bigg*, 1999; *Leck and Svensson*, 2015; *Leck et al*., 2002; *Nilsson et al*., 2001] short-term intensive studies measured the direct flux of particles from leads over the pack ice. However, significant uncertainty remains regarding the extent leads currently influence Arctic particle mass concentrations over multiple seasons and at coastal locations. Therefore, to build on previous work on the production of aerosols from leads and to probe the wind dependence of sea salt aerosol production from Arctic leads across multiple seasons and years, we present an examination of sea salt concentrations near Barrow, Alaska, under varying local sea ice and wind speed conditions from April 2006 to December 2009.

2. Methods

2.1. Meteorology

Wind speed and wind direction data were available with 1 min resolution for the National Oceanic and Atmospheric Administration (NOAA) Barrow Observatory (71°32′30″N, 156°61′14″W) at 10 m above ground. Given that wind speeds $\geq 4\ m\ s^{-1}$ over open ocean are typically associated with the formation of bubbles responsible for sea salt aerosol production [*Monahan and O'Muircheartaigh*, 1986], wind speed data were divided into three average wind speed categories: (1) "low" $< 4\ m\ s^{-1}$, (2) "moderate" 4–7 $m\ s^{-1}$, and (3) "high" $> 7\ m\ s^{-1}$. As there are no direct measurements of wind speed over the adjacent Arctic Ocean available, it is assumed that local measured wind speed is representative of the wind speed over the nearby sea ice and open water. The local wind speeds observed in this study are consistent with previous observations of Arctic wind speeds over sea ice [*Tjernström et al*., 2012], with low or moderate wind speeds present for 22% and 62% of supermicron, respectively, and 29% and 48%, respectively, of submicron particle sampling periods.

2.2. Sea Ice Radar

The coverage of local near-shore sea ice at Barrow, AK was determined by examination of radar backscatter maps (http://seaice.alaska.edu/gi/data/barrow_radar) produced from a Furuno 10 kW, X-band marine radar, which provides high spatial resolution sea ice imaging during both light and dark periods (Figure 1). The radar operated atop a building in downtown Barrow (71°17′33″ N, 156°47′17″W) 22.5 m above sea level, with a range of up to 11 km to the northwest [*Druckenmiller et al*., 2009; *Eicken et al*., 2011]. While the radar only covered sea ice conditions to the northwest in this analysis, any lead activity observed within the 11 km range analyzed in this study was assumed to reflect lead activity along the coast to the southwest and northeast, as observed frequently by *Mahoney et al*. [2014]. Radar backscatter maps were manually analyzed to divide the observed local sea surface into three categories: (1) full sea ice cover present, when local sea ice cover was complete and no areas of exposed ocean surface were present; (2) leads present, when local sea ice cover with areas of exposed ocean surface was present: and (3) open ocean, when no major local sea ice cover was observed on the radar map (Figure 1).

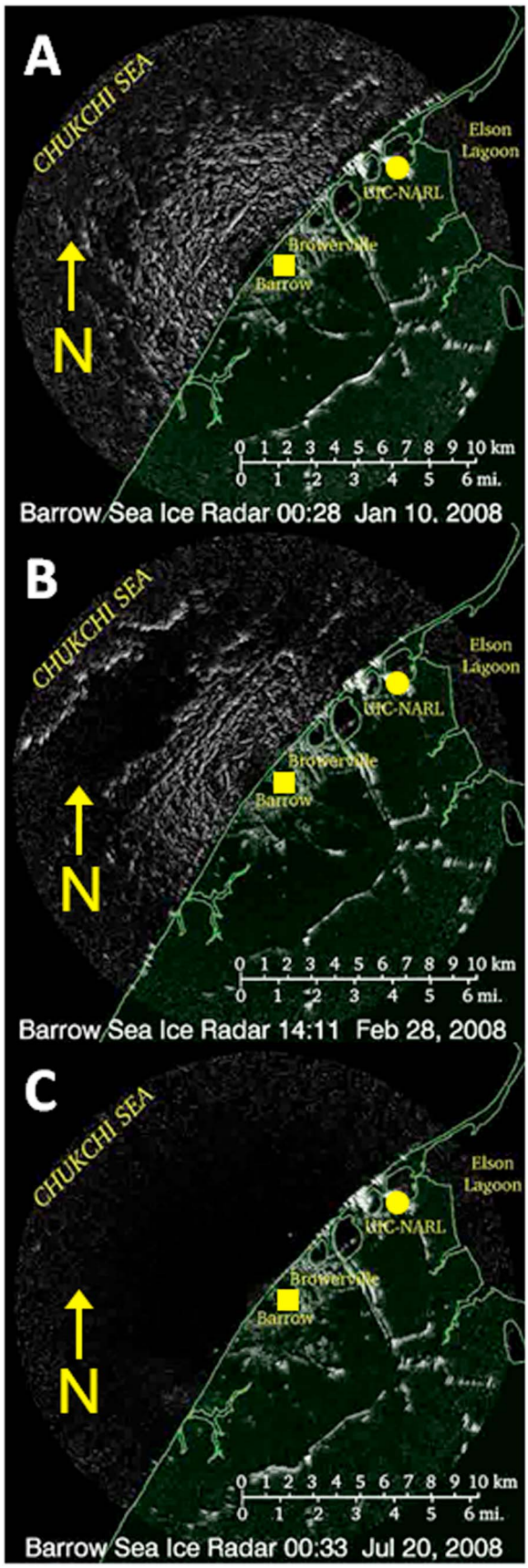

Figure 1. Representative radar backscatter maps of local near-shore sea surface at Barrow, AK. The yellow arrow indicates direction of north, the aerosol sampling location is marked by a yellow circle, and the radar backscatter location is marked with a yellow square. Land is colored green, white is indicative of sea ice, and black is shown for open water. Sea ice conditions include (a) full sea ice coverage, indicated by the full coverage of the white signal indicative of sea ice; (b) leads present, identified from the area of dark signal in the upper left indicative of open ocean present in the middle of the white signal indicative of sea ice; and (c) open ocean, identified from the full coverage of the dark signal indicative of open ocean.

2.3. Aerosol Chemical Composition

Atmospheric particles were sampled at the NOAA Barrow Observatory 10 m above the surface from April 2006 to December 2009. Real-time wind direction was used to sample only from the clean air sector (0°–129°) to avoid influence from local pollution [*Quinn et al.*, 2002]. The Beaufort and Chukchi Seas are 2–25 km upwind of the aerosol sampling site in the clean air sector, so all air sampled is assumed to be of direct marine origin. A Berner-type multijet cascade impactor operating at a sample flow rate of 30 L min^{-1} with 50% cut points at aerodynamic diameters (D_{50}) of 10 μm and 1 μm was used to collect particles with aerodynamic diameters < 1 μm (referred to as submicron particles) and 1–10 μm (referred to as supermicron particles). Particles with diameters < 1 μm passed through an impactor to a rotating filter carousel housing eight Millipore Fluoropore filters (1.0 mm pore size). For every revolution of the rotating submicron filter carousel, seven filters were sampled individually, with sampling time varying depending on season and particle loadings, and one filter, exposed to ambient air for 10 s, served as a blank. Particles with aerodynamic diameters between 1 and 10 μm were collected on Tedlar films over the course of one revolution of the rotating submicron filter carousel, with one additional film collected as a blank for every supermicron sample

collected. To minimize bounce of large particles onto downstream submicron filters, a 12 mm grease cup coated with silicone grease and a film coated with silicone spray were placed on the 10 μm jet [*Quinn et al*., 2002]. Sample air was heated to maintain a stable reference relative humidity (RH) of 40% despite changes in ambient RH. The stable sampling RH allows for a constant instrumental size segregation, and all measurements are reported at the reference RH [*Quinn et al*., 2002]. Submicron and supermicron particle sampling periods ranged from 1 to 11 days and 5 to 35 days, respectively. After collection, sealed filters and films were shipped to the NOAA Pacific Marine Environmental Laboratory for analysis.

For inorganic ion analysis, filters and films were first wetted with 1 mL of spectral grade methanol. Five milliliters of distilled deionized water was then added to the solution, and the samples were extracted by sonicating for 30 min. Concentrations of major cations (Na^+, NH_4^+, K^+, Mg^{2+}, and Ca^{2+}) and anions ($CH_3SO_3^-$, Cl^-, Br^-, NO_3^-, SO_4^{2-}, and $C_2O_4^{2-}$) extracted from each submicron and supermicron particle sample were measured by ion chromatography [*Quinn et al*., 1998]. Details of the inlet, sampling procedures, and chemical analyses can be found in *Delene and Ogren* [2002] and *Quinn et al*. [2002]. Based on the aerosol sampling flow rate (30 L min^{-1}) and typical sampling time, the detection limits calculated as 2 times the standard deviation of the blank for the major sea salt ions of interest, Na^+ and Cl^-, were both 0.0002 μg m^{-3}. For periods that were below the detection limit, a value of half the detection limit (0.0001 μg m^{-3}) was substituted for calculations. Periods below the detection limit constituted 0% of supermicron and 12% submicron sampling periods for Na^+ and 3% of supermicron and 20% submicron sampling periods for Cl^-. Na^+ mass concentration is a conservative tracer for sea salt mass [*Legrand et al*., 2016] and will be discussed henceforth in the place of sea salt mass to avoid biases from varying chloride depletion. While sea spray aerosol is a complex mixture of inorganic salts and organic compounds, the distribution of which alters the chemical and physical properties of the particle, sea spray aerosol is primarily (>60%) composed of inorganic salt [*Quinn et al*., 2015]. All Na^+ is assumed to be derived from seawater [*Quinn et al*., 2002], as *Sirois and Barrie* [1999] showed that the majority of Na^+ in the Arctic is associated with sea salt aerosol. Error was calculated as the standard error of the mean and is not shown for periods when only one sampling period fell into the given sea surface and wind speed category.

3. Results and Discussion

3.1. Sea Salt Mass Concentrations

A clear dependence of supermicron (1–10 μm) Na^+ (sea salt) mass concentrations on the combination of local sea ice coverage and wind speed was observed (Figure 2a). There was little difference in the supermicron Na^+ mass concentrations observed for periods with no leads present and low (<4 m s^{-1}) (0.04 ± 0.01 μg m^{-3}) or moderate (4–7 m s^{-1}) (0.03 μg m^{-3}) wind speeds compared to periods with leads and low wind speeds (0.026 ± 0.009 μg m^{-3}). However, for periods characterized by moderate wind speeds, supermicron Na^+ mass concentrations were higher when leads were present (0.11 ± 0.03 μg m^{-3}) compared to when full sea ice cover was present (0.03 μg m^{-3}). Unfortunately, no supermicron sampling periods of full sea ice coverage with high wind speeds (>7 m s^{-1}) were present for comparison to periods of leads present with high wind speeds.

When leads were present, supermicron Na^+ mass concentrations were 4 and 10 times greater for periods with moderate (0.11 ± 0.03 μg m^{-3}) and high (0.3 ± 0.1 μg m^{-3}) wind speeds, respectively, in comparison to low wind speeds (0.03 ± 0.01 μg m^{-3}) (Figure 2a). This is consistent with wind-driven sea salt aerosol number fluxes from leads observed directly by *Nilsson et al*. [2001] and *Leck et al*. [2002]. Local leads, when observed by the sea ice radar, are the most likely source for the wind-dependent supermicron Na^+ mass observed in this study, as the lifetime of supermicron aerosols in the boundary layer is typically < 12 h [*Williams et al*., 2002]. The short lifetime of these supermicron particles limits the distance from which the majority of these particles could have originated, for the wind speeds observed, to a scale of a few hundred kilometers, which would fall within the area of Arctic sea ice coverage in the winter-spring and for which the sea ice radar is representative of ice fracturing conditions [*Mahoney et al*., 2014].

The highest supermicron Na^+ mass concentrations are expected for open ocean and high wind speeds, as sea salt aerosol production generally increases with increasing wind speed and fetch [*Lewis and Schwartz*, 2004]. While no supermicron particle sampling periods occurred for open ocean and low wind speeds, periods of

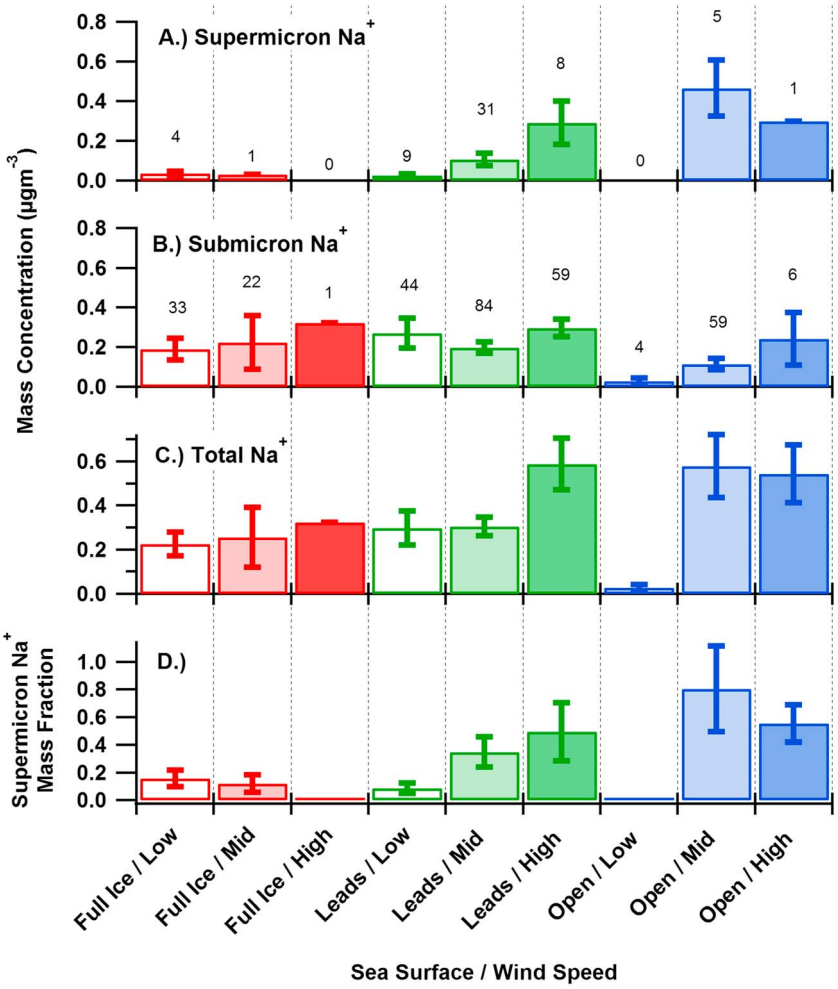

Figure 2. Average mass concentrations of Na^+ for the (a) supermicron (1–10 μm), (b) submicron particle (<1 μm) and (c) total size ranges, and (d) the fraction of the total Na^+ mass that was observed in the supermicron size range, separated into nine bins based on local sea ice extent and wind speed. Sea ice extent categories include full ice, leads present, and open water. Wind speed categories include low (<4 m s^{-1}), mid (4–7 m s^{-1}), and high (>7 m s^{-1}). All error bars were calculated as the standard error of the mean, and the numbers above each category indicate the number of samples in that category.

open ocean with moderate wind speeds showed supermicron Na^+ mass concentrations (0.5 ± 0.1 μg m^{-3}) 5 times greater than for periods when leads were present with moderate winds. Previously, sea salt aerosol number fluxes over leads were measured to be 10 times smaller than those over the open ocean at similar wind speeds, an observation which was attributed to the smaller fetch and area of exposed water [*Leck et al.*, 2002; *Nilsson et al.*, 2001]. Therefore, these long-term measurements show that while a smaller source than open water, leads are a significant wind-dependent source of supermicron sea salt particle mass in the Arctic. The supermicron Na^+ mass concentration for high wind speeds (0.3 μg m^{-3}) was slightly lower than for periods of open ocean with moderate winds (0.5 ± 0.1 μg m^{-3}), contrary to that expected based on the dependence of sea salt aerosol mass over open ocean on wind speed [*Lewis and Schwartz*, 2004]. However, only one open ocean aerosol sampling period was characterized by sustained high winds, imparting uncertainty in the trend that can be attributed to the small sample size and natural variability in meteorological conditions that would impact sea salt aerosol concentrations through deposition and marine boundary layer mixing [*Lewis and Schwartz*, 2004]. However, it is important to note that despite these confounding factors there are statistically significant trends overall in the dependence of supermicron sea salt concentrations on local sea ice extent and local wind speed.

There was no overall dependence of submicron (<1 μm) Na^+ mass concentrations on local sea ice coverage and wind speed (Figure 2b). Unlike supermicron Na^+ mass concentrations, submicron Na^+ mass concentrations did not increase substantially when leads were present. The average submicron Na^+ mass concentration when leads were present was $0.25 \pm 0.03\ \mu g\ m^{-3}$, compared to $0.21 \pm 0.06\ \mu g\ m^{-3}$ when leads were not present. In further contrast to supermicron Na^+ mass concentrations, a wind speed dependence in submicron Na^+ mass concentration was not observed when leads were present (Figure 2b). In fact, open ocean periods with low or moderate wind speeds resulted in the lowest observed submicron Na^+ mass concentrations ($0.03 \pm 0.02\ \mu g\ m^{-3}$ and $0.11 \pm 0.03\ \mu g\ m^{-3}$, respectively). The lack of correlation of submicron Na^+ mass concentrations with local sea ice coverage and wind speed is most likely due to the longer atmospheric residence time of submicron sea salt particles, compared to supermicron sea salt particles [*Gong et al*., 2002; *Williams et al*., 2002]. The shorter residence time of supermicron sea salt aerosol decreases the influence of long-range transport, which significantly influenced the observed submicron sea salt aerosol, as discussed in section 3.2. The long-range transport of submicron sea salt aerosol produced from high-latitude open ocean sources to the Arctic could therefore have a significant influence on submicron Na^+ mass concentrations, as previously concluded [*Barrie and Barrie*, 1990; *Barrie et al*., 1994; *Quinn et al*., 2002; *Sirois and Barrie*, 1999; *Sturges and Barrie*, 1988].

During periods of full sea ice cover and open ocean, submicron Na^+ mass concentrations exhibited a correlation with wind speed. For full sea ice periods, submicron Na^+ mass concentrations increased from low ($0.19 \pm 0.05\ \mu g\ m^{-3}$) and moderate ($0.2 \pm 0.1\ \mu g\ m^{-3}$) to high wind speed ($0.3\ \mu g\ m^{-3}$), although the increase from moderate to high wind speed was not statistically significant, in part due to the availability of only one sampling period at high wind speed for comparison (Figure 2b). Under full ice conditions, a non–wave breaking source of Na^+, as discussed in section 3.4, could potentially contribute, in addition to long-range transport, as discussed in section 3.2. For open ocean periods, submicron Na^+ showed a greater dependence on local meteorology. Submicron Na^+ mass concentrations increased from low ($0.03 \pm 0.01\ \mu g\ m^{-3}$) to moderate ($0.11 \pm 0.03\ \mu g\ m^{-3}$) and high ($0.2 \pm 0.1\ \mu g\ m^{-3}$) wind speeds. However, the increase from moderate to high wind speeds was not statistically significant. The higher sea salt concentrations under these open ocean conditions, along with the decrease in the fraction of aged submicron sea salt periods discussed in section 3.2, suggests the influence of submicron sea salt production from local wind-driven wave breaking processes.

Overall, the supermicron fraction of the total Na^+ mass concentration increased with decreasing sea ice coverage and, in the presence of leads, increasing wind speed (Figures 2c and 2d). Supermicron Na^+ mass concentrations comprised less than 20% of the total Na^+ mass concentrations for periods with full sea ice cover and with leads and low winds. In the presence of leads, the supermicron Na^+ mass fraction increased with increasing wind speed. At moderate wind speeds the supermicron Na^+ mass concentration comprised 40% of the total Na^+ mass concentration for periods with leads, ~4 times greater than periods with leads and low wind speeds. Then, for periods with leads and high wind speeds, the supermicron Na^+ mass fraction increased to 50% of the total Na^+ mass concentration. Finally, the supermicron Na^+ mass fraction was the most dominant for periods with open ocean, comprising 60–80% of the total Na^+ mass concentration. The dependence of supermicron Na^+ mass fraction on local sea ice coverage and wind speed highlights that the supermicron sea salt aerosol population is more directly influenced by local sea ice coverage and wind speed than the submicron sea salt aerosol population, as expected due to the longer atmospheric residence time of submicron sea salt particles [*Gong et al*., 2002; *Williams et al*., 2002].

3.2. Contributions of Aged Sea Salt Aerosol

Cl^-/Na^+ molar ratios were calculated to investigate sea salt aerosol lifetime and chemical processing, a measure of the influence of long-range transport. Sea salt aerosol retains the Cl^-/Na^+ molar ratio of seawater (1.16) when introduced into the atmosphere [*Keene et al*., 1986]. This ratio is altered in the atmosphere through the displacement of chlorine through reaction with acidic gases, such as H_2SO_4, or aqueous oxidation of $SO_{2(g)}$ [*Keene et al*., 1998]. The extent of aging is thus dependent on atmospheric residence time, as well as the original particle mass and acidic precursor concentrations in the atmosphere [*Leck et al*., 2002]. Previous work has shown that fine sea salt aerosol (aerodynamic diameter < 2.5 μm) are more likely to have greater chloride depletion than those of larger diameter coarse (aerodynamic diameter > 2.5 μm) sea salt aerosol [*Barrie et al*., 1994; *Hara et al*., 2002; *Leck et al*., 2002]. In addition, previous work has shown that sea

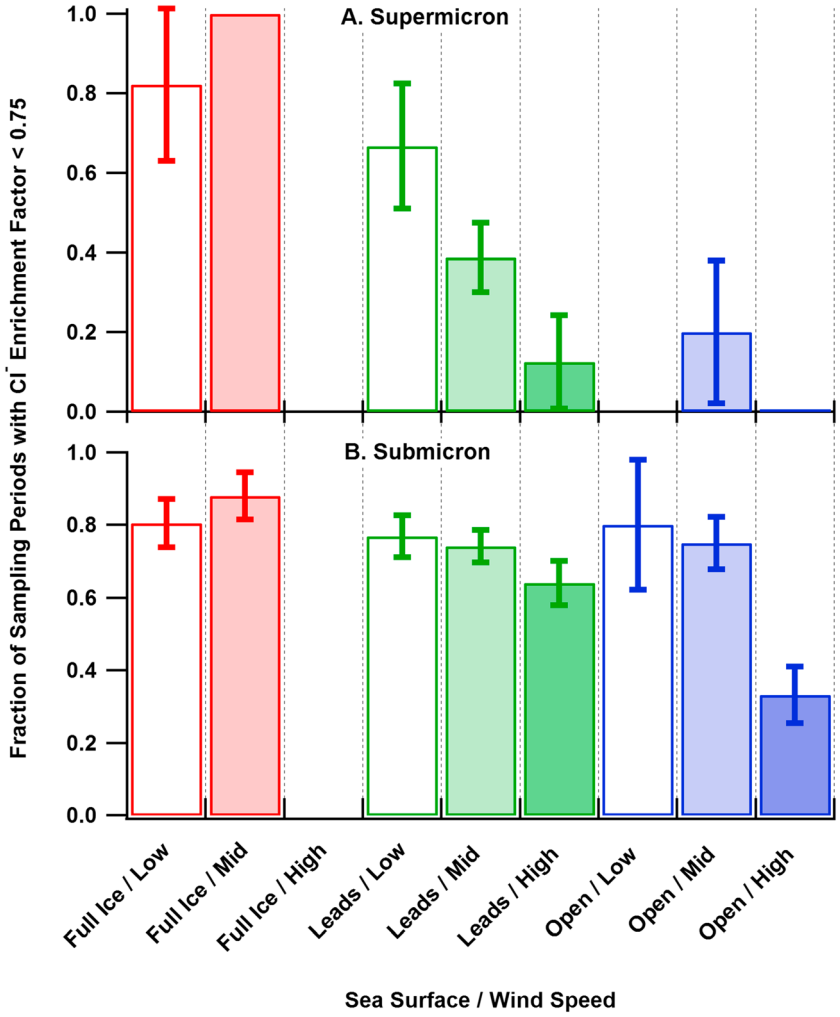

Figure 3. The fraction of sampling periods with a Cl^- enrichment factor < 0.75, corresponding to aged sea salt for (a) supermicron and (b) submicron size ranges, divided into categories based on sea ice conditions and wind speed, similar to Figure 2.

salt aerosols exhibit greater depletion following polar sunrise when production of sulfuric acid from the oxidation of $SO_{2(g)}$ occurs in the Arctic troposphere [*Sirois and Barrie*, 1999]. Using Cl^-/Na^+ molar ratios (Figure S1 in the supporting information), fractions of sampling periods dominated by "aged" sea salt were calculated for each sea ice and wind speed category (Figure 3). Aged sea salt was defined as having a Cl^- enrichment factor < 0.75. Cl^- enrichment factor is determined by dividing the Cl^-/Na^+ ratio of the aerosol sample by the Cl^-/Na^+ ratio of bulk seawater [*Newberg et al.*, 2005]. Therefore, an enrichment factor < 0.75 corresponds to the depletion of 25% or more of Cl^- from sea salt aerosol and represents particles that have undergone significant atmospheric processing. Sampling periods with a Cl^-/Na^+ enrichment factor > 0.75 were considered to consist primarily of "fresh" sea salt produced from local sources.

The average fraction of aged submicron sea salt periods (0.74 ± 0.07) across all local sea ice coverage and wind speed categories was higher than the fraction of aged supermicron sea salt periods (0.39 ± 0.06) (Figure 3). The median Cl^-/Na^+ molar ratios for submicron and supermicron sea salt aerosol sampling periods also exhibited a dependence on local sea ice coverage and wind speed (Figure S2). Overall, the median Cl^-/Na^+ molar ratio of submicron sea salt periods (0.62) was lower than the median Cl^-/Na^+ molar ratio for supermicron sampling periods (0.86) (Figure S2). This indicates that the atmospheric processing undergone by the submicron sea salt resulted in a greater Cl^- depletion than the supermicron sea salt, as expected since smaller particles have a longer residence time [*Williams et al.*, 2002] and a higher surface area to volume ratio [*McInnes et al.*, 1994].

The highest fractions (0.7–0.8) of aged sea salt sampling periods were observed when full sea ice cover with low and moderate wind speeds were present, consistent with the lack of a local sea salt source (Figure 3). The fractions of aged submicron and supermicron sea salt periods when leads or open ocean were present with low wind speed were similarly high (0.6–0.8). That some of the highest fractions of aged sea salt were observed under low wind conditions across all sea ice coverage categories indicates that the sea salt observed during low wind periods, regardless of sea ice coverage, experienced increased atmospheric processing, likely due to long-range transport.

For periods with leads present, the fraction of aged submicron and supermicron sea salt periods, respectively, decreased from low (0.77 ± 0.06; 0.7 ± 0.2) to moderate (0.74 ± 0.05; 0.39 ± 0.09) to high wind speeds (0.64 ± 0.06; 0.1 ± 0.1), consistent with greater contributions from a wind-dependent local sea salt aerosol source (Figure 3). However, this potential decrease in the fraction of aged submicron sea salt periods with increased wind speed, when leads were present, was partly within error. When open ocean was present, the fraction of aged submicron sea salt periods decreased, partly within error, with increasing wind speed (low wind speed = 0.8 ± 0.2; moderate wind speed = 0.75 ± 0.07; high wind speed = 0.3 ± 0.1), again consistent with a wind-dependent local sea salt aerosol source. These trends in sea salt aging are consistent with local sea salt aerosol production increasing with decreasing local sea ice coverage and increasing wind speed. This further supports wind-driven sea salt aerosol production, dominated by supermicron particles, from leads.

3.3. Difference in Particle Production From Leads Versus Open Ocean

In addition to differences in particle lifetime between submicron and supermicron sea salt aerosol [*Williams et al*., 2002], differences in the production mechanisms of submicron and supermicron sea salt aerosol from leads likely also contributed to the observed trends in aged fractions and sea salt mass fractions. *Leck et al*. [2002] and *Nilsson et al*. [2001] hypothesized that compared to open ocean production, film drop particle production from leads depends less on wind speed than jet drop particle production. As a result, the sea salt aerosol size distribution over pack ice is dominated by a larger particle diameter lognormal mode at ~2 μm, while over open ocean, a smaller particle diameter lognormal mode centered at 100 nm dominates [*Nilsson et al*., 2001]. This is consistent with the lognormal size distribution of sea salt aerosol resulting from film and jet drops centered at ~100–200 nm and ~1–2 μm dry diameters, respectively, measured by *O'Dowd et al*. [1997]. Thus, the larger contribution of fresh supermicron sea salt, compared to submicron sea salt, observed during periods with leads and moderate to high winds (Figure 3) is consistent with the hypothesis that jet drops are the dominant production mechanism of sea salt aerosol from leads. Additionally, the increased presence of smaller particles over open ocean observed by *Nilsson et al*. [2001] is evident in this study by the increased presence of fresh submicron sea salt during periods of open ocean and high wind speeds (Figure 3). These results therefore suggest that the differences in wind-driven production of sea salt aerosol from leads, compared to open ocean, shift the mass distribution of sea salt aerosol in the Arctic toward larger sizes when leads are present. This could impact radiative forcing and cloud processes in the Arctic as CCN efficiency is size dependent [*Dusek et al*., 2006].

3.4. Non–Wave Breaking Particle Sources

Sea salt aerosol production from local leads and open ocean appears to be the dominant contributor to sea salt mass concentrations in this study. However, submicron sea salt mass concentrations, sampled under conditions where local sea salt aerosol production are not expected (e.g., $0.21 \pm 0.06\ \mu g\ m^{-3}$ when full sea ice cover was present), were equal to or greater than those from other categories where local sea salt production are expected (e.g., $0.12 \pm 0.03\ \mu g\ m^{-3}$ when open ocean was present). This suggests that there were sea salt aerosol sources even when no exposed ocean surface was present (Figure 2b). Frost flowers, highly saline ice crystals grown on rapidly freezing open leads, are a potential source for wind-driven sea salt aerosol production when no open ocean is present [*Rankin et al*., 2000]. However, as discussed in the supporting information, the contribution from wind-blown frost flowers to the measured sea salt aerosol concentrations was likely minor as there were no full sea ice cover sampling periods with SO_4^{2-}/Na^+ molar ratios indicative of frost flowers (<0.02) (Figure S3) [*Douglas et al*., 2012]. In comparison, SO_4^{2-}/Na^+ molar ratios for fresh seawater and fresh sea salt aerosol are ~0.06 [*Keene et al*., 2007]. However, sulfate isotope analysis would be necessary to fully determine the influence of frost flowers, as anthropogenic sulfates can mask the sulfate depleted frost flower sea salt [*Norman et al*., 1999; *Seguin et al*., 2014]. High winds can also loft saline snow particles, which are suggested to form aerosols by sublimation [*Lieb-Lappen and Obbard*, 2015;

Yang et al., 2008]. The increase in submicron Na^+ mass concentrations from low wind speed ($0.19 \pm 0.05\ \mu g\ m^{-3}$), to moderate wind speed ($0.2 \pm 0.1\ \mu g\ m^{-3}$), to high wind speed ($0.3\ \mu g\ m^{-3}$) for periods with full sea ice cover was not also observed in the supermicron Na^+ mass concentrations. Therefore, additional detailed field measurements of aerosol size and chemical composition are required to examine the potential size-dependent production of aerosols from blowing snow. However, this increase in submicron Na^+ mass concentration was within error. In addition, the Cl^-/Na^+ ratio of blowing snow in Barrow, AK, is expected to be similar to the ocean water ratio [*Jacobi et al.*, 2012], such that any fresh sea salt observed during full ice periods can potentially be attributed to this source. Therefore, with less than 30% of the full sea ice cover submicron and supermicron sampling periods characterized by fresh sea salt, the contribution from blowing snow production to the observed Na^+ mass concentrations is likely minor with transported sea salt aerosol representing a greater contribution.

3.5. Seasonality of Sea Salt Aerosol Production

The Arctic sea ice coverage undergoes seasonal changes, with growth during winter, loss during summer, and pack ice movement due to winds and currents [*Mahoney et al.*, 2014]. In this study, particle sampling periods with local full sea ice cover occurred during the months of November through June (Figure S4). For these months, 11–36% and 0–25% of all submicron and supermicron particle sampling periods, respectively, corresponded to local full sea ice coverage. For Barrow, AK, *Quinn et al.* [2002] previously observed a winter maximum in submicron sea salt aerosol, attributed to long-range transport from high-latitude regions of the Pacific and Atlantic Oceans with seasonally high winds. This is consistent with the observations of the highest fractions of aged sea salt and submicron Na^+ mass concentrations during sampling periods with full sea ice cover, suggesting that the winter sea salt aerosol population had the longest transport time from its source. As expected, open ocean near Barrow was observed between July and November (Figure S4). The minimum fractions of aged sea salt and maximum supermicron Na^+ mass concentrations were observed during these periods of local open ocean, suggesting the sea salt aerosol population during summer had the shortest transport time from its source. The lower particle dry deposition velocity, and resulting longer particle lifetime, over sea ice compared to over open ocean in the Arctic [*Nilsson and Rannik*, 2001] likely also contributed to the higher fraction of aged sea salt and higher submicron Na^+ mass concentrations during sampling periods with full sea ice cover compared to periods of local open ocean. Nearby leads were observed to be present between October and July and were the dominant sea ice category over the entire study (Figure S3). Supermicron particle sampling periods with leads present comprised 50–91% of the supermicron particle sampling periods months of October to July. Submicron particle sampling periods with leads present comprised 64–91%, and 5%, of submicron particle sampling periods November to July, and October, respectively. This suggests that sea salt aerosol production from leads currently impacts sea salt aerosol mass concentrations, especially in the supermicron particle size range, in the Arctic atmosphere throughout the majority of the year.

4. Conclusions

This three-year study at Barrow, AK allowed a comprehensive investigation into the influences of sea ice coverage and wind speed on sea salt mass concentrations in the coastal Arctic. Wind-driven production of sea salt aerosol from leads contributes significantly to sea salt aerosol mass concentrations in the Arctic, but to a lesser extent than wind-driven production of sea salt aerosol from open ocean. This is consistent with previous short-term summertime number flux measurements of sea salt aerosol over open leads, where sea salt aerosol emissions were ~10 times smaller than the open ocean [*Leck et al.*, 2002; *Nilsson et al.*, 2001]. The influence of sea salt aerosol production from open leads was most apparent in the supermicron size range, as evidenced by the strong dependence on wind speed of supermicron sea salt mass concentrations, which increased by a factor of 10 from periods with low wind speed to periods with high wind speeds, when leads were present. The increase in supermicron Na^+ mass concentration from $0.035 \pm 0.007\ \mu g\ m^{-3}$, when leads were not present, to $0.12 \pm 0.02\ \mu g\ m^{-3}$ when leads were present, provides further evidence of the influence of sea salt aerosol production from leads. There was evidence of wind-driven submicron sea salt production from local leads, but submicron sea salt, depleted in chloride, from long-range transport comprised the majority (~70%) of the submicron sea salt mass. The influence of long-range transport was greatest when local sea salt aerosol production would not be expected, including periods of low winds and full sea ice cover.

This improves our knowledge of complex atmosphere-sea ice feedbacks [*Shepson et al*., 2012]. Supermicron sea salt aerosol production from leads could increase direct radiative forcing, as supermicron sea salt can contribute significantly to scattering in the remote marine boundary layer [*Quinn et al*., 1998]. This supermicron sea salt aerosol could also impact indirect radiative forcing and cloud properties as giant CCN (2–10 μm), which can induce the formation of larger cloud droplets and accelerate precipitation in the presence of smaller particles [*Yin et al*., 2000]. The CCN response to supermicron sea salt aerosol produced from leads may be reduced by the efficient removal of large particles in the highly scavenging nature of the Arctic atmosphere, particularly in summer [*Browse et al*., 2012]. Supermicron sea salt aerosol emissions from leads would also increase the atmospheric condensation sink, which is predicted to suppress particle nucleation from dimethyl sulfide and reduce total CCN concentrations [*Browse et al*., 2014]. Increased emissions of supermicron sea salt aerosol from leads thus could play an important role in controlling the CCN response to changes in sea ice [*Browse et al*., 2014]. Supermicron sea salt aerosol could also alter snowpack and atmospheric halogen photochemistry, and therefore atmospheric oxidation [*Simpson et al*., 2005]. The impacts of wind-driven production of sea salt aerosol from leads could be particularly evident in winter and early spring when sea ice coverage is at its maximum and submicron sea salt mass concentrations are typically higher than supermicron sea salt mass concentrations due to a lack of local open ocean source [*Quinn et al*., 2002]. Given decreasing multiyear sea ice extent and increasing ice fracturing [*Stroeve et al*., 2012], wind-driven production of supermicron sea salt aerosol from leads could therefore increase the supermicron sea salt aerosol mass fraction in the Arctic in the winter-spring, changing the annual contributions of sea salt aerosol to the Arctic winter and early spring [*Sirois and Barrie*, 1999] may further increase the atmospheric sea salt mass burden [*Browse et al*., 2012]. To fully understand the influence of sea salt aerosol produced from leads, measurements of sea salt aerosol concentrations with higher time resolution must be combined with sea ice coverage measurements that take into account a larger area. Furthermore, to understand the long-term impacts of changing sea ice on the Arctic, decadal comparisons between sea ice conditions and sea salt aerosol are necessary.

Acknowledgments

The University of Michigan College of Literature, Science, and the Arts is thanked for funding this analysis. Hajo Eicken of the Sea Ice Group at the Geophysical Institute at the University of Alaska Fairbanks is thanked for discussions regarding, and assistance in obtaining, the sea ice radar backscatter maps. We thank the NOAA personnel at Barrow, AK for sample collection and Kristen Schulz (NOAA PMEL) for sample analysis. NOAA Barrow Observatory meteorological and aerosol data are available online (http://www.esrl.noaa.gov/gmd/obop/brw/), and Barrow sea ice radar backscatter maps can be found online at http://seaice.alaska.edu/gi/data/barrow_radar. The PMEL contribution number is 4408.

References

Barrie, L. A., and M. J. Barrie (1990), Chemical components of lower tropospheric aerosols in the high arctic: Six years of observations, *J. Atmos. Chem.*, *11*, 211–226.

Barrie, L. A., R. Staebler, D. Toom, B. Georgi, G. Denhartog, S. Landsberger, and D. Wu (1994), Arctic aerosol size-segregated chemical observations in relation to ozone depletion during Polar Sunrise Experiment 1992, *J. Geophys. Res.*, *99*(D12), 25,439–25,451, doi:10.1029/94JD01514.

Blanchard, D. C., and A. H. Woodcock (1957), Bubble formation and modification in the sea and its meteorological significance, *Tellus*, *9*(2), 145–158, doi:10.1111/j.2153-3490.1957.tb01867.x.

Boucher, O., et al. (2013), Clouds and aerosols, in *Climate Change 2013: The Physical Science Basis. Contribution of Working Group I to the Fifth Assessment Report of the Intergovernmental Panel on Climate Change*, edited by T. F. Stocker et al., pp. 571–658, Cambridge Univ. Press, Cambridge, U. K., and New York.

Browse, J., K. S. Carslaw, S. R. Arnold, K. Pringle, and O. Boucher (2012), The scavenging processes controlling the seasonal cycle in Arctic sulphate and black carbon aerosol, *Atmos. Chem. Phys.*, *12*(15), 6775–6798, doi:10.5194/acp-12-6775-2012.

Browse, J., K. S. Carslaw, G. W. Mann, C. E. Birch, S. R. Arnold, and C. Leck (2014), The complex response of Arctic aerosol to sea-ice retreat, *Atmos. Chem. Phys.*, *14*(14), 7543–7557, doi:10.5194/acp-14-7543-2014.

Delene, D. J., and J. A. Ogren (2002), Variability of aerosol optical properties at four North American surface monitoring sites, *J. Atmos. Sci.*, *59*(6), 1135–1150, doi:10.1175/1520-0469(2002)059<1135:voaopa>2.0.co;2.

Douglas, T. A., et al. (2012), Frost flowers growing in the Arctic ocean-atmosphere-sea ice-snow interface: 1. Chemical composition, *J. Geophys. Res.*, *117*, D00R09, doi:10.1029/2011JD016460.

Druckenmiller, M. L., H. Eicken, M. A. Johnson, D. J. Pringle, and C. C. Williams (2009), Toward an integrated coastal sea-ice observatory: System components and a case study at Barrow, Alaska, *Cold Reg. Sci. Technol.*, *56*(2–3), 61–72, doi:10.1016/j.coldregions.2008.12.003.

Dusek, U., et al. (2006), Size matters more than chemistry for cloud-nucleating ability of aerosol particles, *Science*, *312*(5778), 1375–1378, doi:10.1126/science.1125261.

Eicken, H., J. Jones, R. Mv, C. Kambhamettu, F. J. Meyer, A. Mahoney, and M. L. Druckenmiller (2011), Environmental security in arctic ice-covered seas: From strategy to tactics of hazard identification and emergency response, *Mar. Technol. Soc. J.*, *45*(3), 37–48.

Gong, S. L., L. A. Barrie, and M. Lazare (2002), Canadian Aerosol Module (CAM): A size-segregated simulation of atmospheric aerosol processes for climate and air quality models—2. Global sea-salt aerosol and its budgets, *J. Geophys. Res.*, *107*(D24), 4779, doi:10.1029/2001JD002004.

Grammatika, M., and W. B. Zimmerman (2001), Microhydrodynamics of flotation processes in the sea surface layer, *Dyn. Atmos. Oceans*, *34*(2–4), 327–348, doi:10.1016/S0377-0265(01)00073-2.

Hara, K., K. Osada, K. Matsunaga, Y. Iwasaka, T. Shibata, and K. Furuya (2002), Atmospheric inorganic chlorine and bromine species in Arctic boundary layer of the winter/spring, *J. Geophys. Res.*, *107*(D18), 4361, doi:10.1029/2001JD001008.

Held, A., I. M. Brooks, C. Leck, and M. Tjernström (2011a), On the potential contribution of open lead particle emissions to the central Arctic aerosol concentration, *Atmos. Chem. Phys.*, *11*, 3093-3105, doi:10.5194/acp-11-3093-2011.

Held, A., D. A. Orsini, P. Vaattovaara, M. Tjernström, and C. Leck (2011b), Near-surface profiles of aerosol number concentration and temperature over the Arctic Ocean, *Atmos. Meas. Tech.*, *4*(8), 1603–1616, doi:10.5194/amt-4-1603-2011.

Jacobi, H. W., D. Voisin, J. L. Jaffrezo, J. Cozic, and T. A. Douglas (2012), Chemical composition of the snowpack during the OASIS spring campaign 2009 at Barrow, Alaska, *J. Geophys. Res.*, *117*, D00R13, doi:10.1029/2011JD016654.

Johnson, B. D., and P. J. Wangersky (1987), Microbubbles: Stabilization by monolayers of adsorbed particles, *J. Geophys. Res.*, *92*(C13), 14,641–14,647, doi:10.1029/JC092iC13p14641.

Keene, W. C., A. A. P. Pszenny, J. N. Galloway, and M. E. Hawley (1986), Sea-salt corrections and interpretation of constituent ratios in marine precipitation, *J. Geophys. Res.*, *91*(D6), 6647–6658, doi:10.1029/JD091id06p06647.

Keene, W. C., R. Sander, A. A. P. Pszenny, R. Vogt, P. J. Crutzen, and J. N. Galloway (1998), Aerosol pH in the marine boundary layer, *J. Aerosol Sci.*, *29*(3), 339–356, doi:10.1016/s0021-8502(97)10011-8.

Keene, W. C., et al. (2007), Chemical and physical characteristics of nascent aerosols produced by bursting bubbles at a model air-sea interface, *J. Geophys. Res.*, *112*, D21202, doi:10.1029/2007JD008464.

Leck, C., and C. Persson (1996), Seasonal and short-term variability in dimethyl sulfide, sulfur dioxide and biogenic sulfur and sea salt aerosol particles in the arctic marine boundary layer during summer and autumn, *Tellus B*, *48*(2), doi:10.3402/tellusb.v48i2.15891.

Leck, C., and E. K. Bigg (1999), Aerosol production over remote marine areas—A new route, *Geophys. Res. Lett.*, *26*(23), 3577–3580, doi:10.1029/1999GL010807.

Leck, C., and E. Svensson (2015), Importance of aerosol composition and mixing state for cloud droplet activation over the Arctic pack ice in summer, *Atmos. Chem. Phys.*, *15*(5), 2545–2568, doi:10.5194/acp-15-2545-2015.

Leck, C., M. Norman, E. K. Bigg, and R. Hillamo (2002), Chemical composition and sources of the high Arctic aerosol relevant for cloud formation, *J. Geophys. Res.*, *107*, 4135, doi:10.1029/2001JC001463.

Legrand, M., X. Yang, S. Preunkert, and N. Theys (2016), Year-round records of sea salt, gaseous, and particulate inorganic bromine in the atmospheric boundary layer at coastal (Dumont d'Urville) and central (Concordia) East Antarctic sites, *J. Geophys. Res. Atmos.*, *121*, 997–1023, doi:10.1002/2015JD024066.

Lewis, E. R., and S. E. Schwartz (2004), *Sea Salt Aerosol Production: Mechanisms, Methods, Measurements, and Models—A Critical Review*, AGU, Washington, D. C.

Lieb-Lappen, R. M., and R. W. Obbard (2015), The role of blowing snow in the activation of bromine over first-year Antarctic sea ice, *Atmos. Chem. Phys.*, *15*(13), 7537–7545, doi:10.5194/acp-15-7537-2015.

Mahoney, A. R., H. Eicken, A. G. Gaylord, and R. Gens (2014), Landfast sea ice extent in the Chukchi and Beaufort Seas: The annual cycle and decadal variability, *Cold Reg. Sci. Technol.*, *103*, 41–56, doi:10.1016/j.coldregions.2014.03.003.

Maslanik, J., J. Stroeve, C. Fowler, and W. Emery (2011), Distribution and trends in Arctic sea ice age through spring 2011, *Geophys. Res. Lett.*, *38*, L13502, doi:10.1029/2011GL047735.

McInnes, L. M., D. S. Covert, P. K. Quinn, and M. S. Germani (1994), Measurements of chloride depletion and sulfur enrichment in individual sea-salt particles collected from the remote marine boundary layer, *J. Geophys. Res.*, *99*(D4), 8257, doi:10.1029/93JD03453.

Monahan, E. C., and I. G. O'Muircheartaigh (1986), Whitecaps and the passive remote sensing of the ocean surface, *Int. J. Remote Sens.*, *7*(5), 627–642, doi:10.1080/01431168608954716.

Newberg, J. T., B. M. Matthew, and C. Anastasio (2005), Chloride and bromide depletions in sea-salt particles over the northeastern Pacific Ocean, *J. Geophys. Res.*, *110*, D06209, doi:10.1029/2004JD005446.

Nilsson, E. D., and Ü. Rannik (2001), Turbulent aerosol fluxes over the Arctic Ocean: 1. Dry deposition over sea and pack ice, *J. Geophys. Res.*, *106*, 32,125-32,137, doi:10.1029/2000JD900605.

Nilsson, E. D., U. Rannik, E. Swietlicki, C. Leck, P. P. Aalto, J. Zhou, and M. Norman (2001), Turbulent aerosol fluxes over the Arctic Ocean: 2. Wind-driven sources from the sea, *J. Geophys. Res.*, *106*(D23), 32,139–32,154, doi:10.1029/2000JD900747.

Norman, A. L., L. A. Barrie, D. Toom-Sauntry, A. Sirois, H. R. Krouse, S. M. Li, and S. Sharma (1999), Sources of aerosol sulphate at Alert: Apportionment using stable isotopes, *J. Geophys. Res.*, *104*(D9), 11,619–11,631, doi:10.1029/1999JD900078.

Norris, S. J., I. M. Brooks, G. de Leeuw, A. Sirevaag, C. Leck, B. J. Brooks, C. E. Birch, and M. Tjernström (2011), Measurements of bubble size spectra within leads in the Arctic summer pack ice, *Ocean Sci.*, *7*(1), 129–139, doi:10.5194/os-7-129-2011.

O'Dowd, C. D., M. H. Smith, I. E. Consterdine, and J. A. Lowe (1997), Marine aerosol, sea-salt, and the marine sulphur cycle: A short review, *Atmos. Environ.*, *31*(1), 73–80, doi:10.1016/s1352-2310(96)00106-9.

Overland, J. E., and M. Wang (2013), When will the summer Arctic be nearly sea ice free?, *Geophys. Res. Lett.*, *40*, 2097–2101, doi:10.1002/grl.50316.

Pratt, K. A., et al. (2013), Photochemical production of molecular bromine in Arctic surface snowpacks, *Nat. Geosci.*, *6*(5), 351–356, doi:10.1038/ngeo1779.

Quinn, P. K., D. J. Coffman, V. N. Kapustin, T. S. Bates, and D. S. Covert (1998), Aerosol optical properties in the marine boundary layer during the first Aerosol Characterization Experiment (ACE 1) and the underlying chemical and physical aerosol properties, *J. Geophys. Res.*, *103*(D13), 16,547–16,563, doi:10.1029/97JD02345V.

Quinn, P. K., D. B. Collins, V. H. Grassian, K. A. Prather, and T. S. Bates (2015), Chemistry and related properties of freshly emitted sea spray aerosol, *Chem. Rev.*, *115*(10), 4383–4399, doi:10.1021/cr500713g.

Quinn, P. K., T. L. Miller, T. S. Bates, J. A. Ogren, E. Andrews, and G. E. Shaw (2002), A 3-year record of simultaneously measured aerosol chemical and optical properties at Barrow, Alaska, *J. Geophys. Res.*, *107*, 4130, doi:10.1029/2001JD001248.

Radke, L. F., P. V. Hobbs, and J. E. Pinnons (1976), Observations of cloud condensation nuclei, sodium-containing particles, ice nuclei and the light-scattering coefficient near Barrow, Alaska, *J. Appl. Meteorol.*, *15*(9), 982–995, doi:10.1175/1520-0450(1976)015<0982:ooccns>2.0.co;2.

Rankin, A. M., V. Auld, and E. W. Wolff (2000), Frost flowers as a source of fractionated sea salt aerosol in the polar regions, *Geophys. Res. Lett.*, *27*(21), 3469–3472, doi:10.1029/2000GL011771.

Salter, M. E., P. Zieger, J. C. Acosta Navarro, H. Grythe, A. Kirkevåg, B. Rosati, I. Riipinen, and E. D. Nilsson (2015), An empirically derived inorganic sea spray source function incorporating sea surface temperature, *Atmos. Chem. Phys.*, *15*(19), 11,047–11,066, doi:10.5194/acp-15-11047-2015.

Scott, W. D., and Z. Levin (1972), Open channels in sea ice (leads) as ion sources, *Science*, *177*(4047), 425–426, doi:10.1126/science.177.4047.425.

Seguin, A. M., A.-L. Norman, and L. Barrie (2014), Evidence of sea ice source in aerosol sulfate loading and size distribution in the Canadian High Arctic from isotopic analysis, *J. Geophys. Res. Atmos.*, *119*, 1087–1096, doi:10.1002/2013JD020461.

Serreze, M. C., and J. Stroeve (2015), Arctic sea ice trends, variability and implications for seasonal ice forecasting, *Philos. Transact. A Math. Phys. Eng. Sci.*, *373*(2045), doi:10.1098/rsta.2014.0159.

Shepson, P. B., et al. (2012), Changing polar environments: Interdisciplinary challenges, *Eos Trans. AGU*, *93*(11), 117, doi:10.1029/2012EO110001.

Simpson, W., L. Alvarez-Aviles, T. A. Douglas, M. Sturm, and F. Domine (2005), Halogens in the coastal snow pack near Barrow, Alaska: Evidence for active bromine air-snow chemistry during springtime, *Geophys. Res. Lett.*, *32*, L04811, doi:10.1029/2004GL021748.

Sirois, A., and L. A. Barrie (1999), Arctic lower tropospheric aerosol trends and composition at Alert, Canada: 1980–1995, *J. Geophys. Res.*, *104*(D9), 11,599, doi:10.1029/1999JD900077.

Stroeve, J., M. Serreze, M. Holland, J. Kay, J. Malanik, and A. Barrett (2012), The Arctic's rapidly shrinking sea ice cover: A research synthesis, *Clim. Change*, *110*(3–4), 1005–1027, doi:10.1007/s10584-011-0101-1.

Struthers, H., A. M. L. Ekman, P. Glantz, T. Iversen, A. Kirkevag, E. M. Martensson, O. Seland, and E. D. Nilsson (2011), The effect of sea ice loss on sea salt aerosol concentrations and the radiative balance in the Arctic, *Atmos. Chem. Phys.*, *11*(7), 3459–3477, doi:10.5194/acp-11-3459-2011.

Sturges, W. T., and L. A. Barrie (1988), Chlorine, bromine and iodine in Arctic aerosols, *Atmos. Environ.*, *22*(6), 1179–1194, doi:10.1016/0004-6981(88)90349-6.

Tjernström, M., et al. (2012), Meteorological conditions in the central Arctic summer during the Arctic Summer Cloud Ocean Study (ASCOS), *Atmos. Chem. Phys.*, *12*(15), 6863–6889, doi:10.5194/acp-12-6863-2012.

Williams, J., M. de Reus, R. Krejci, H. Fischer, and J. Ström (2002), Application of the variability-size relationship to atmospheric aerosol studies: estimating aerosol lifetimes and ages, *Atmos. Chem. Phys.*, *2*(2), 133–145, doi:10.5194/acp-2-133-2002.

Wise, M. E., E. J. Freney, C. A. Tyree, J. O. Allen, S. T. Martin, L. M. Russell, and P. R. Buseck (2009), Hygroscopic behavior and liquid-layer composition of aerosol particles generated from natural and artificial seawater, *J. Geophys. Res.*, *114*, D03201, doi:10.1029/2008JD010449.

Yang, X., J. A. Pyle, and R. A. Cox (2008), Sea salt aerosol production and bromine release: Role of snow on sea ice, *Geophys. Res. Lett.*, *35*, L16815, doi:10.1029/2008GL034536.

Yin, Y., Z. Levin, T. G. Reisin, and S. Tzivion (2000), The effects of giant cloud condensation nuclei on the development of precipitation in convective clouds—A numerical study, *Atmos. Res.*, *53*(1–3), 91–116, doi:10.1016/s0169-8095(99)00046-0.